Accepted Manuscript

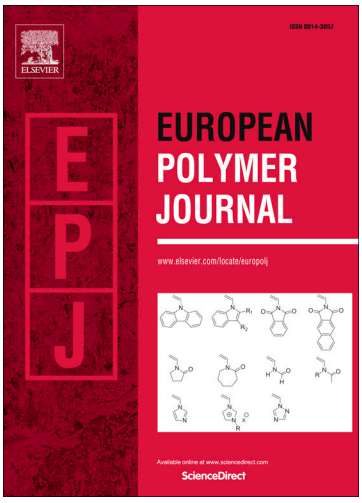

Ionically conducting and photoresponsive liquid crystalline terpolymers: towards multifunctional polymer electrolytes

Laura Vanti, Sakinah Mohd Alauddin, Daniel Zaton, Nurul Fadhilah Kamalul Aripin, Marco Giacinti-Baschetti, Corrie T. Imrie, Amparo Ribes-Greus, Alfonso Martinez-Felipe

PII: S0014-3057(18)31041-3
DOI: https://doi.org/10.1016/j.eurpolymj.2018.08.033
Reference: EPJ 8546

To appear in: *European Polymer Journal*

Received Date: 6 June 2018
Revised Date: 19 July 2018
Accepted Date: 19 August 2018

Please cite this article as: Vanti, L., Mohd Alauddin, S., Zaton, D., Fadhilah Kamalul Aripin, N., Giacinti-Baschetti, M., Imrie, C.T., Ribes-Greus, A., Martinez-Felipe, A., Ionically conducting and photoresponsive liquid crystalline terpolymers: towards multifunctional polymer electrolytes, *European Polymer Journal* (2018), doi: https://doi.org/10.1016/j.eurpolymj.2018.08.033

Ionically conducting and photoresponsive liquid crystalline terpolymers: towards multifunctional polymer electrolytes.

Laura Vanti[1], Sakinah Mohd Alauddin[2], Daniel Zaton[3,4], Nurul Fadhilah Kamalul Aripin[2], Marco Giacinti-Baschetti[1], Corrie T. Imrie[4], Amparo Ribes-Greus[5] and Alfonso Martinez-Felipe[3,*]

[1]Department of Civil, Chemical, Environmental, and Materials Engineering, Università degli studi Bologna, Via Terracini 34 40131 Bologna, Italy.

[2] Faculty of Chemical Engineering, University of Technology MARA, 40450 Shah Alam, Selangor Darul Ehsan, Malaysia.

[3]Chemical and Materials Engineering Group, School of Engineering, University of Aberdeen, King's College, Aberdeen AB24 3UE, Scotland, UK.

[4]Chemistry, School of Natural and Computing Sciences, Meston Building, University of Aberdeen, Aberdeen AB24 3UE, Scotland, UK.

[5]Institute of Materials Technology, Universidad Politécnica de Valencia, Camino de Vera S/N, 46022 Valencia, Spain.

*corresponding author: a.martinez-felipe@abdn.ac.uk

Keywords: side-chain liquid crystal polymers; polymer electrolytes; light responsive materials.

ABSTRACT

We have prepared a series of new ionically conducting polymer electrolytes consisting of side-chain liquid crystal terpolymers with mesogenic azobenzenes, sulfonic acid groups and methyl methacrylate. The poly[10-(4-methoxyazobenzene -4'-oxy)decyl methacrylate]-co-poly[2-acrylamido-2-methyl-1-propanesulfonic acid]-co-poly[methyl methacrylate]s, 10-MeOAzB/AMPS/MMA terpolymers, were synthesised by a one-pot conventional radical polymerisation. All samples were characterised by NMR, GPC/SEC, FT-IR, POM, XRD, DSC, UV-visible spectrophotometry and EIS. The terpolymers have light responsive properties, and exhibit liquid crystallinity over a wide range of compositions. Above a certain threshold of AMPS content, the 10-MeOAzB/AMPS/MMA terpolymers exhibit ionic conductivities in the 10^{-8}-10^{-4} S·cm^{-1} range, with signs of decoupling of ionic mobility from segmental motions of the polymer.

1. INTRODUCTION

Polymer electrolytes are at the core of several electrochemical devices, and are particularly attractive for low temperature applications due to their relative low cost and high versatility. By chemical and physical modification, it is possible to yield new polymer electrolytes with a broad range of functionalities designed to control transport properties.[1] Effective ion and charge transport through the electrolyte is needed to optimise energy conversion and storage in batteries, fuel cells, electrolysers or supercapacitors,[2] but the design of polymeric membranes is also crucial for other analytical and purification technologies.[3] The performance of some benchmark polymer electrolytes, however, depends on the presence of phase separated morphologies between polar and non-polar regions promoted by the presence of solvents, making it difficult to optimise the ion transport without altering other properties.[4]

Thermotropic liquid crystals offer alternative mechanisms to control the morphology of polymer electrolytes.[5] Their anisotropic response to external stimuli, such as mechanical shearing, light, or magnetic and electrical fields, can be used to create preferential pathways for molecular and ion transport. In recent years, a wide variety of 1D-columnar, 2D-planar and 3D-bicontinuous liquid crystalline materials have been proposed as components in batteries, fuel cells and actuators.[6] Liquid crystallinity, for example, may inhibit the crystallisation of poly(ethylene oxide), which has been extensively used as an electrolyte for lithium ion batteries, thus increasing the mobility of lithium ions and cell performance.[7-9] Poly(imides) with planar alignments,[10, 11] and calamitic and discotic electrolytes with columnar suprastructures,[12] on the other hand, have been explored to facilitate anisotropic proton conductivity in fuel cell electrolytes. Self-assembly of liquid crystals has also proved to be useful to develop nanostructured sensors, and to yield multi-responsive poly(electrolytes), where pH, temperature and light have synergetic effects on conductivity.[13-17] In these applications, the fluidity of the mesophases can promote local mobility, as occurs

in ionic liquids and polymerised ionic liquids,[18-21] but with the potential of the anisotropic control of transport.

Recently, we have studied the phase behaviour and structure of new side-chain liquid crystal polymers containing sulfonic acid groups, as potential components in ionically conducting polymer electrolytes.[22-24] Microphase separation between the backbone and the side groups confines the polar groups between smectic layers, resulting in potential anisotropic ionic pathways.[25-27] The strong interactions between the sulfonic acid groups, however, disrupt, at least to some extent, the formation of liquid crystalline phases, and restrict the compositional range over which mesogenic behaviour is observed in these materials.[28, 29]

In the present work, we investigate the effect of including methyl methacrylate, as a third non-mesogenic/non-ionic component, on the structure and conductivity of new side-chain terpolymers containing sulfonic acid and azobenzene units, the poly[10-(4-methoxyazobenzene -4'-oxy)decyl methacrylate]-co-poly[2-acrylamido-2-methyl-1-propanesulfonic acid]-co-poly[methylmethacrylate]s, 10-MeOAzB/AMPS/MMA terpolymers, ***1***,

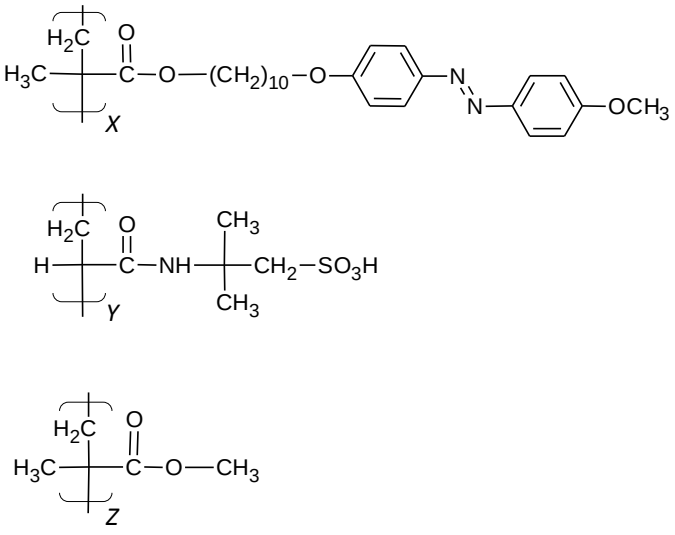

1

With the introduction of methacrylate units, we aim to regulate the interactions involving the conducting and mesogenic components, and promote the formation of different ultrastructures that may enhance the conductivity and film forming properties of these materials. The presence of the azobenzene-based groups will allow control of their macroscopic properties using light stimuli *via* changes in the local order.[15, 30-36]

2. EXPERIMENTAL SECTION

Synthesis and materials

The 10-MeOAzB/AMPS/MMA terpolymers, ***1***, were prepared over a broad range of compositions of the corresponding monomers: (i) the mesogenic side chains, 10-(4-methoxyazobenzene -4'-oxy)decyl methacrylate, 10-MeOAzB, (ii) polar groups for solvating ions, acrylamido-2-methyl-1-propanesulfonic acids, AMPS, and (iii) methyl(methacrylate) groups, MMA, as non-mesogenic/non-ionic structure modifying units.

AMPS and MMA were commercially available from Sigma-Aldrich and used without further purification. 10-MeOAzB was prepared according to a procedure described in detail elsewhere.[37-39] The 10-MeOAzB/AMPS/MMA terpolymers were prepared using a one-pot conventional free radical polymerisation under an inert atmosphere and appropriate amounts of the different monomers.[40] Further details of the synthetic procedure are provided in the Electronic Supplementary Information, **ESI.**

Characterisation techniques

The chemical structures of all the terpolymers and their intermediates were verified using ^{1}H-NMR, and Fourier transform infrared, FT-IR, spectroscopies. ^{1}H-NMR spectra were measured using either a Gemini 300 analyser or a 300 MHz Bruker Ultrashield NMR spectrometer, in either $CDCl_3$ or DMSO-d_6. FT-IR spectra were obtained using a Thermo Nicolet 5700 spectrometer for sample discs containing around 1 mg of product and 200 mg of potassium bromide (KBr, ~ 0.5 % by weight), prepared using a Specac 15 ton manual hydraulic press. The spectra were collected in Absorbance (Abs, %) units as the average of 64 scans, in the 4000 – 400 cm^{-1} range, and with 4 cm^{-1} resolution. A background spectrum for a pristine KBr disc was measured before each series of experiments. Molecular weights

and polydispersities of the polymers were assessed by gel permeation/size exclusion chromatography, GPC/SEC, using a Waters 1515 module with a refractive index detector (Waters 2414). Samples were eluted in tetrahydrofuran with a flow rate of 1 ml/min at 40ºC. Molecular weight calibration was performed using polystyrene standards.

The phase behaviour of the terpolymers was studied by polarised light microscopy, POM, using an Olympus BH-2 optical microscope equipped with a Linkam THMS 600 heating stage and a TMS 91 control unit, and the thermal transitions were determined by differential scanning calorimetry, DSC, using a Mettler Toledo DSC 822 analyser. Samples of around 5 mg were heated from 25ºC to 220ºC, held at 220ºC for 3 minutes, cooled to 25ºC, held for 3 minutes, and re-heated to 220ºC. All the scans were performed at $10^{o}C \cdot min^{-1}$ under a nitrogen atmosphere and using liquid nitrogen as the coolant. The thermal stability of the samples was assessed by thermogravimetric analysis, TGA, using a Mettler Toledo TGA/SDTA 851 modulus. Around 5 mg of sample in an Al_2O_3 pan containing a hole for gas release were heated from room temperature to 750ºC, at $10^{o}C \cdot min^{-1}$, under inert argon atmosphere with a flow rate of 200 $ml \cdot min^{-1}$.

X-ray diffraction, XRD, patterns were obtained using a Bruker AXS D8 Discover X-ray diffractometer equipped with a Hi-Star 2D detector with CuKα-radiation filtered by cross-coupled Göbel mirrors at 40 kV and 40 mA. Samples were mounted on a piece of Scotch tape, heated to 150ºC, cooled slowly to room temperature, and their diffraction pattern recorded. The sample to detector distance was set to 13 cm and calibration of this distance was carried out using silver behenate as the reference. Molecular lengths were estimated using ACD/ChemSketch. The light-responsive character of the 10-MeOAzB/AMPS/MMA terpolymers was assessed by measuring the UV-visible absorption spectra at room temperature in solution and films, and further details are given as Supplementary Information.

Ionic conductivity was measured using a Hioki 3532-50 LCR Hi tester in the frequency range of 50 Hz to 5 MHz, between 303 and 423 K. A few mg of the terpolymer were melted on a stainless steel electrode (20 mm diameter, SUS316), allowed to cool slowly into the liquid crystal phase, covered with a second similar electrode, and then further cooled to room temperature. The electrodes were separated by a Teflon ring of internal diameter 12 mm. Samples were heated above their clearing point inside the cell, and then measured in isothermal steps on cooling to room temperature. The results were obtained in terms of the complex dielectric permittivity, $\varepsilon^* = \varepsilon' - i\varepsilon''$, which was transformed into the complex impedance, Z^*, and conductivity, σ^*, using:

$$Z^* = Z' + iZ'' = \frac{1}{i\omega C_0 \varepsilon^*}$$

and

$$\sigma^* = i\ \omega\varepsilon_0\varepsilon^*$$

where i is the imaginary unit, ω is the angular frequency in $\mathrm{rad}\cdot\mathrm{s}^{-1}$, C_0 is the cell capacitance and ε_0 is the permittivity in the vacuum, $8.854x10^{-12}\ \frac{\mathrm{F}}{\mathrm{m}}$.

.

3. RESULTS AND DISCUSSION

Composition and molecular weight analysis

We refer to the 10-MeOAzB/AMPS/MMA terpolymers as A*X*/S*Y*/M*Z*, where *X*, *Y* and *Z* are the molar percentages of 10-MeOAzB, AMPS and MMA, respectively, as assessed experimentally by ^{1}H-NMR spectroscopy. Specifically, we calculated the composition in terms of the relative integrals of the 7-8 ppm signals, assigned to the phenyl azobenzene protons (4H) of 10-MeOAzB, the ~2.7 ppm singlet, assigned to the methylene groups (2H) adjacent to the sulfonic acid groups in AMPS, and the peak at ~3.6 ppm, associated with the methyl groups (3H) of MMA. For the sake of comparison, we have divided the terpolymers into two main groups, see **Table 1**. In samples #1 to #4 we keep the concentration of AMPS groups relatively low and vary the amount of MMA groups, whereas in samples #5 to #8 we explore a broader range of AMPS concentrations.

The FT-IR spectra of the terpolymers contain bands characteristic of the functional groups in the individual components, including the carbonyl stretching bands from the ester groups in 10-MeOAzB and MMA (~1730 cm^{-1}) together with the C=O stretching band (~1670 cm^{-1}) and the N-H stretching and bending signals (~3400 and ~1550 cm^{-1}, respectively) from the amide groups in AMPS.[23] These observations are consistent with the proposed chemical structures of the terpolymers, ***1***. The molecular weights of all the terpolymers were measured by gel permeation/size exclusion chromatography, GPC/SEC, and these are also listed in **Table 1**. The degrees of polymerisation, *DP*, are sufficiently high (*DP*>15) to ensure that their transitional properties do not lie in the strongly molecular weight dependent regime and thus comparisons may be made between them.[37] Due to the number of different signals appearing in the $\delta\sim$ 2 - 1 ppm region, it is difficult to determine the existence of cross-correlations between proton signals in the main chain arising from the different repeating units of AMPS (1H, CH_2), 10-MeOAzB, and MMA (CH_3, CH_2), by using 2D correlation

NMR, ^{1}H-COSY, see **Figure ESI2**. Considering that acrylamides show smaller reactivity ratios than methacrylates in radical initiated copolymers [41-44], we cannot rule out that our 10-MeOAzB/AMPS/MMA terpolymers may contain tapered chains initiated by polymerisation of methacrylate units, to which AMPS groups attach, following a statistical distribution.

Table 1. Molecular weights, polydispersities, M_w/M_n, and number average degrees of polymerization, *DP*, for the 10-MeOAzB/AMPS/MMA terpolymers, ***1***. Also listed are the feed compositions used in the copolymerisations. *X*, *Y* and *Z* are the molar percentages of 10-MeOAzB, AMPS and MMA, respectively, assessed experimentally.

Sample	**A*X*/S*Y*/M*Z* Experimental**	**A*X*/S*Y*/M*Z* Feed**	M_n / g·mol^{-1}	M_w / g·mol^{-1}	M_w / M_n	*DP*
	P10-MeOAzB (A100/S0/M0)	100/0/0	12544	27094	2.2	28
#1	A70/S15/M15	72/18/10	17390	60278	3.5	45
#2	A55/S20/M25	48/12/40	16139	47850	3.0	51
#3	A50/S15/M35	64/16/20	13204	28286	2.1	41
#4	A41/S11/M48	32/08/60	14308	31855	2.2	56
#5	A61/S30/M09	63/27/10	35284	784402	22.2	102
#6	A29/S36/M35	33/33/33	12698	83058	6.5	53
#7	A43/S40/M17	45/45/10	13064	48158	3.7	45
#8	A09/S85/M06	36/54/10	15687	212104	13	72

Thermal stability

The thermal stability of the terpolymers was assessed by thermogravimetric analysis, TGA, and the weight loss curves, TG, and corresponding derivative curves, DTG, are shown in **Figures 1(a)** and **1(b)**, respectively. Thermal degradation of the P10-MeOAzB homopolymer occurs through two main weight loss processes, which we attribute to the breaking of the more labile groups in the side chains, between 300ºC and 400ºC, followed by decomposition of the polymer backbone, between 400 ºC and 500ºC.[45, 46]

The residual values of all the polymers under study, after heating to 750ºC, fall within 15 to 20%, in weight %, which are high values compared to PMMA, and these can be explained by the presence of the side chains.[46] In general terms, the terpolymers display a main weight loss around 400ºC, as well as an additional process at about 300ºC, see **Figure 1(b)**. This latter weight loss is presumably associated with the decomposition of the MMA and the AMPS units in the polymer chain. Terpolymers with high AMPS contents (samples #6 to #8) display additional processes below 300ºC, which may, at least in part, be associated with the release of solvent trapped within the polymer structure.[4, 22, 47] Samples exposed to UV-light irradiation during 15 minutes at temperatures within the expected operational conditions (below 150ºC), retained their phase behaviour, and did not show signs of photolytic degradation under the polarised optical microscope, see **ESI**.

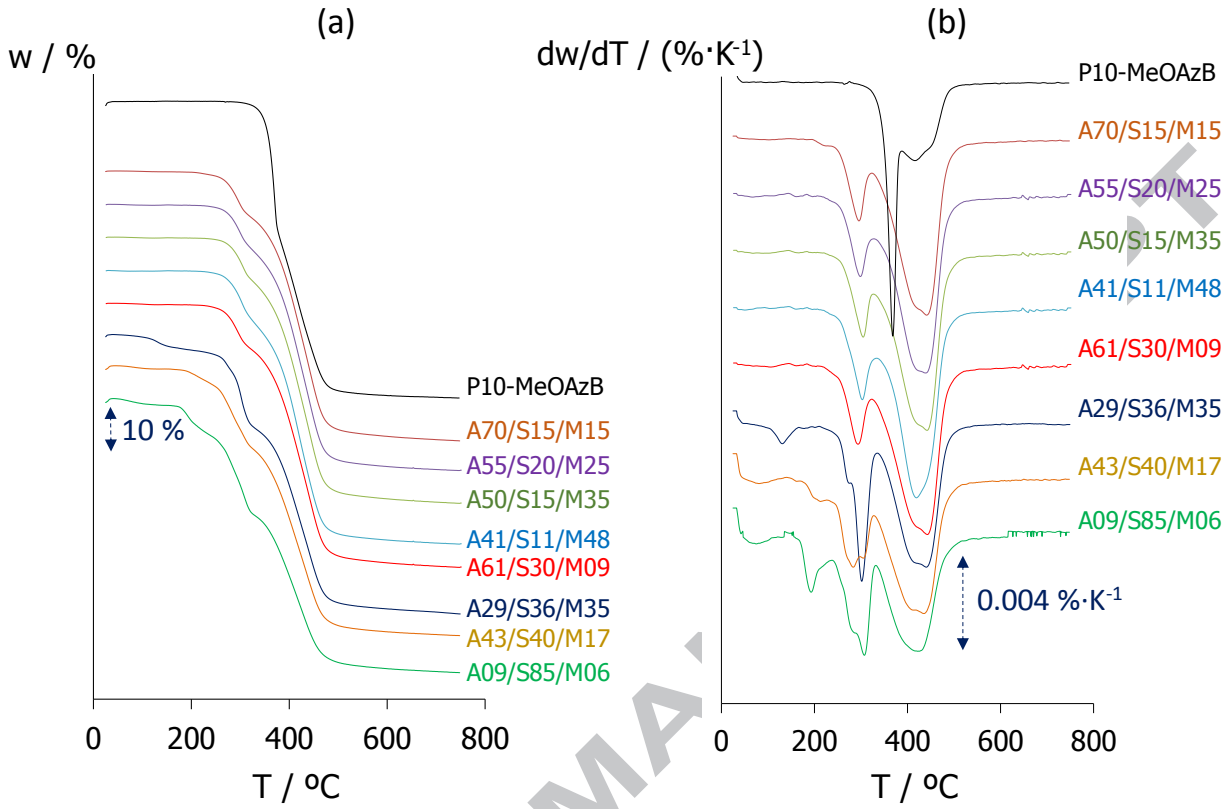

Figure 1. (a) Thermogravimetric curves, TG, and **(b)** derivative thermogravimetric curves, DTG, corresponding to the P10-MeOAzB homopolymer and the 10-MeOAzB/AMPS/MMA terpolymers. Curves have been shifted arbitrarily along the Y-axes.

Phase behaviour

The transitional properties of the terpolymers are listed in **Table 2**. The 10-MeOAzB homopolymer, P10-MeOAzB, exhibits enantiotropic smectic A and nematic behaviour and vitrifies to form a smectic glass. The nematic phase is observed over a very narrow temperature range on cooling from the isotropic melt, and prior to the formation of the smectic A phase.[48] 10-MeOAzB/AMPS/MMA terpolymers with moderate and high concentrations of mesogenic units (≥29%, molar %) also show liquid crystallinity, assigned on the basis of the observation of fluid birefringent regions when viewed through the

polarised optical microscope, POM, see **ESI.** Unfortunately, the optical textures are not well-defined and were not useful for phase assignment.

The DSC traces obtained for the 10-MeOAzB/AMPS/MMA terpolymers for their second heating scans are shown in **Figure 2**. Terpolymers with $A \geq 29\%$ exhibit two distinct thermal events: a glass transition, T_g (between 60 ºC and 80 ºC), and a first order transition at higher temperatures, associated with the liquid crystal to isotropic transition, T_{LCI}, in excellent agreement with observations made using POM. The terpolymers tend to exhibit higher glass transitions than P10-MeOAzB, presumably reflecting the less flexible poly(methyl methacrylate), PMMA (T_g > 100ºC)[49], and PAMPS (T_g~124ºC)[22] backbones. This increase is counteracted, at least to some extent, by a plasticizing effect of the flexible 10-MeOAzB side-chains. The terpolymer with the lowest mesogenic content (A = 9%) is not liquid crystalline, and shows only a glass transition in the DSC trace, again consistent with the POM observation. We note that this T_g is, surprisingly, the lowest of the terpolymers, and we suggest that may be attributed to the lower density of the isotropic phase compared to the liquid crystal phase shown by the other terpolymers, which serves to increase T_g.

Reducing the concentration of mesogenic units in the terpolymers lowers the clearing point with respect to the P10-MeOAzB homopolymer and narrows the liquid crystal temperature ranges. The decrease in T_{LCI} for most of the samples lies between 10 and 18ºC, and does not vary linearly with the concentration of mesogenic units. This is consistent with our previous report that the introduction of moderate amounts of AMPS chains causes only small reductions in T_{LCI} for the 10-MeOAzB/AMPS copolymers.[22] The data listed in **Table 2** indicate that MMA has a destabilising effect on liquid crystalline behaviour, and the sample with the highest MMA concentration, A41/S11/M48, exhibits the lowest T_{LCI}.

Table 2. Transition temperatures and associated enthalpy, ΔH_{LCI}, and entropy, $\Delta S_{LCI}/R$, changes for P10-MeOAzB and the 10-MeOAzB/AMPS/MMA terpolymers. R, gas constant.

Sample	**A*X*/S*Y*/M*Z***	**T_g (ºC)**	**T_{LCI} (ºC)**	**ΔH_{LCI} ($J \cdot g^{-1}$)**	**ΔH_{LCI} ($kJ \cdot mol^{-1}$)**	**$\Delta S_{LCI}/R$**
	P10-MeOAzB* (A100/S0/M0)	71	135	11.22	5.08	1.50
#1	A70/S15/M15	72	125	5.38	2.13	0.64
#2	A55/S20/M25	79	117	6.58	2.30	0.71
#3	A50/S15/M35	76	125	5.59	2.14	0.65
#4	A41/S11/M48	**	97	7.84	2.32	0.75
#5	A61/S30/M09	72	126	5.38	2.13	0.64
#6	A29/S36/M35	82	120	3.08	0.76	0.23
#7	A43/S40/M17	76	128	5.78	2.13	0.64
#8	A09/S85/M06	64	-	-	-	-

* Enthalpy, ΔH_{LCI}, and entropy, $\Delta S/R_{LCI}$, values corresponding to merged isotropic to nematic and nematic to smectic A transitions.[22]

** Overlapped with first-order transition.

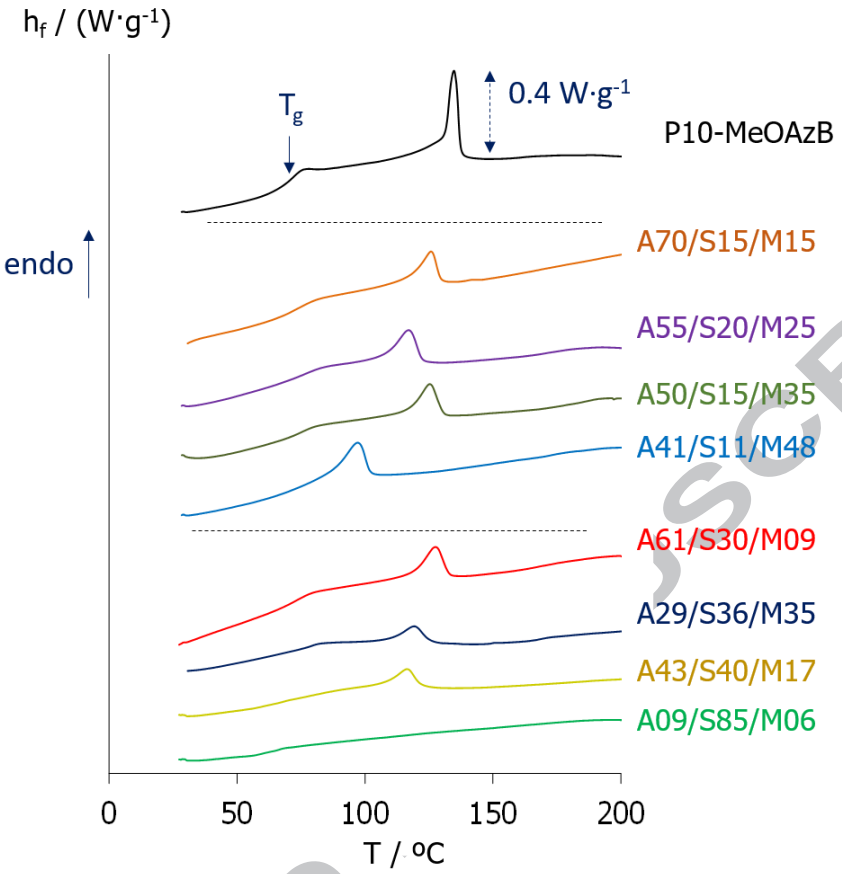

Figure 2. DSC traces corresponding to the second heating scans of the P10-MeOAzB homopolymer and the 10-MeOAzB/AMPS/MMA terpolymers. Curves have been shifted arbitrarily along the Y-axis (h_f, heat flux).

Phase structure

Figure 3 shows the X-ray diffraction patterns of the terpolymers obtained at room temperature after cooling slowly from the isotropic or liquid crystalline phases. The P10-MeOAzB diffractogram in **Figure 3(a)** contains a strong reflection in the small angle region, $2\theta_1 \sim 5.74^o$, and a broad diffuse reflection at wider angles, $2\theta_2 \sim 12^o$. The wider angle reflection corresponds to the periodicity along the polymer backbone (d_2 ~ 7.4 Å). The low-angle reflection corresponds to the smectic periodicity (d_1 ~ 15.7 Å) and is approximately half the length of the mesogenic 10-MeOAzB side chains in all-*trans* conformations, l~ 32

Å. This suggests a fully interleaved smectic A phase (SmA_1), see **Figure 4(a)**.[50] Alternatively, however, the ratio d_1 /l~ 0.5 may reflect a quasi-symmetrical distribution of the electronic density about the mid-point of the smectic layers and the backbone domains.[48]

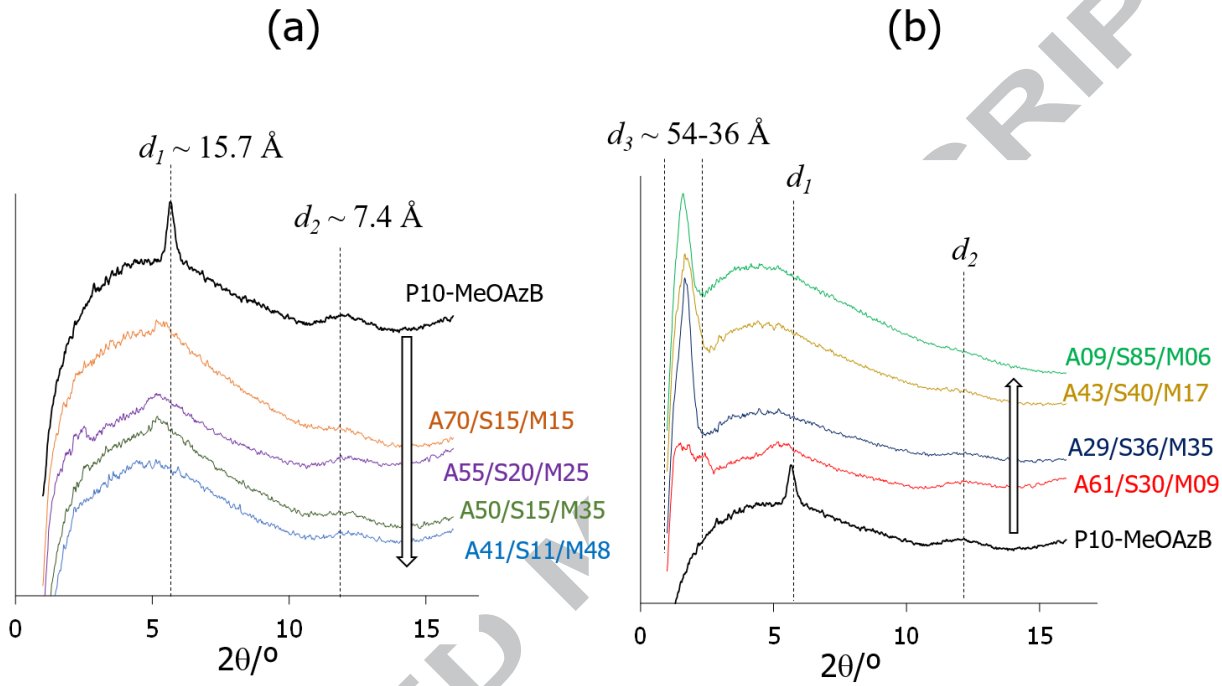

Figure 3. XRD diffraction patterns obtained at room temperature on cooling from the liquid crystal/isotropic phases of P10-MeOAzB (in both images) and the 10-MeOAzB/AMPS/MMA terpolymers. **(a)** Effect of increasing MMA content in samples #1 to #4; **(b)** increasing AMPS content in samples #5 to #8. Arrows indicate decreasing mesogenic content. Y-axes correspond to the diffractogram intensity, *a.u.*, and curves have been shifted arbitrarily along this axis.

The XRD patterns of the terpolymers contain similar reflections in the same small and wide angle regions as described for the pattern of P10-MeOAzB, confirming the phase assignment made by POM, which also is consistent with the magnitudes of the associated enthalpy changes listed in **Table 2**.[50] On increasing MMA content, the intensity of the small angle peak decreases and shifts towards lower 2θ values, **Figure 3(a)**, reflecting the disruption of

the smectic layers arising from the dilution of the mesogenic units. In order to accommodate the increasing number of non-mesogenic units, the polymer backbone of the terpolymers is, at least to some extent, distorted, facilitating interfacial mixing between the main chain and the 10-MeOAzB side groups. This effectively swells the layer giving larger spacings (up to d_1 ~18.3 Å).

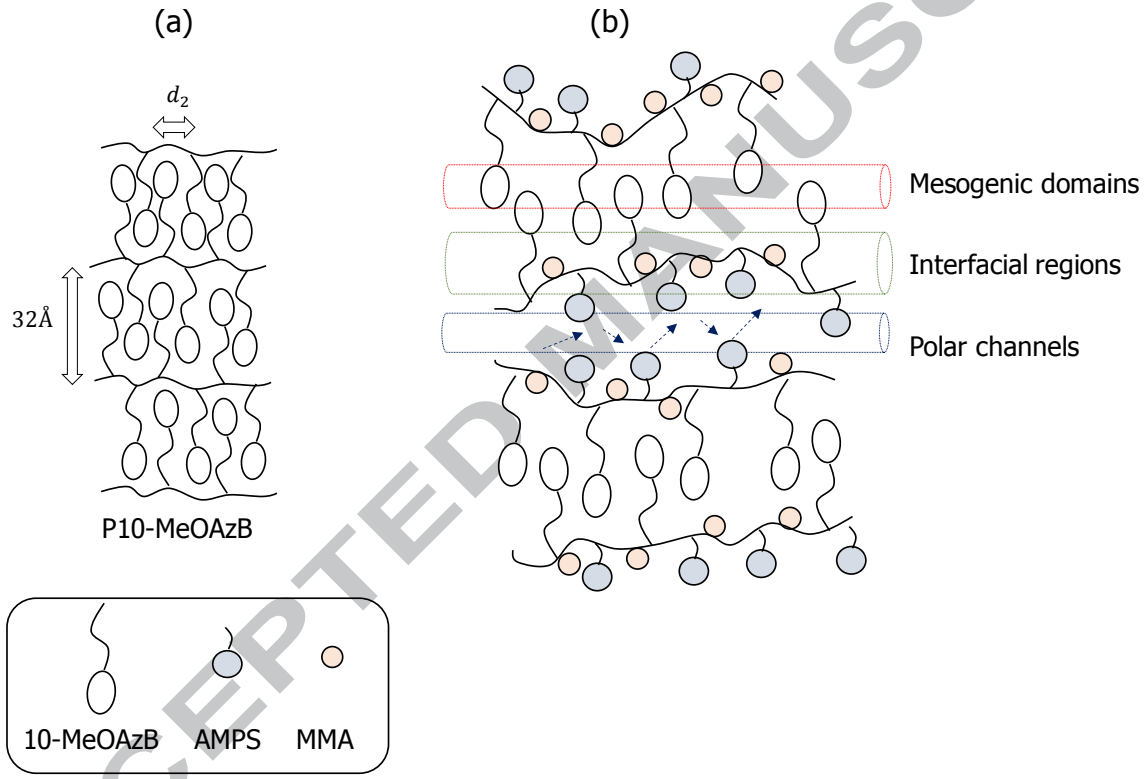

Figure 4. Schematic structural models for the smectic phases shown by **(a)** P10-MeOAzB and **(b)** the 10-MeOAzB/AMPS/MMA terpolymers containing equal amounts of the three components, showing coexisting smectic domains and polar channels. Dotted arrows indicate potential ionically conducting pathways.

The presence of large amounts of AMPS in samples #5 to #8 is associated with the appearance of a strong reflection at small angles, $2\theta_3$~1.70-2.54º, see **Figure 3(b)**, which we

assign to the formation of polar aggregates in the terpolymers.[40] The nature of the interactions involving the AMPS units may be investigated using FT-IR spectroscopy, and the spectra of the terpolymers measured at room temperature are shown in **Figure 5**. It is noteworthy that the O-H stretching (*st*.) region (expected between 3400 and 3500 cm^{-1}) is rather weak and overlaps the stronger N-H *st.* band (ν~3300 cm^{-1}). This suggests that the sulfonic acid groups (SO_3H) in the AMPS units may be, at least partially, deprotonated in the terpolymers.[23] The presence of sulfonate groups is also associated with a new signal assigned to the SO_3^- *st*. vibration in the range 1020 -1040 cm^{-1}, [23] which varies with AMPS contents, **Figure ESI5**.

The appearance of the strong small angle reflection on increasing AMPS content in the terpolymers, **Figure 3**, indicates the co-existence of smectic domains and AMPS-rich regions even at moderate concentrations of AMPS ($S \geq 20\%$, molar). This suggests that the AMPS units are squeezed between alternating smectic layers that are further stabilised by micro-phase separation between polar and non-polar domains, see **Figure 4(b)**. The appearance of the NH *st.* band in **Figure 5** at relatively low frequencies ($\nu < 3400$ cm^{-1}) and the presence of Fermi bands in the vicinity of ν ~2500 cm^{-1}, are indicative of the existence of extensive hydrogen bonding near the backbone.[51-54] Such strong interactions may further contribute to stabilise the smectic order by constraining the mobility of the neighbouring 10-MeOAzB side chains.[24, 28] The methyl methacrylate units in the terpolymers may weaken the interactions between the AMPS groups located in the backbone, mitigating to some extent these stabilising effects, and promoting broader transition peaks in **Figure 2**. All these features may reflect some interfacial mixing between AMPS and 10-MeOAzB domains in these terpolymers.[55-57]

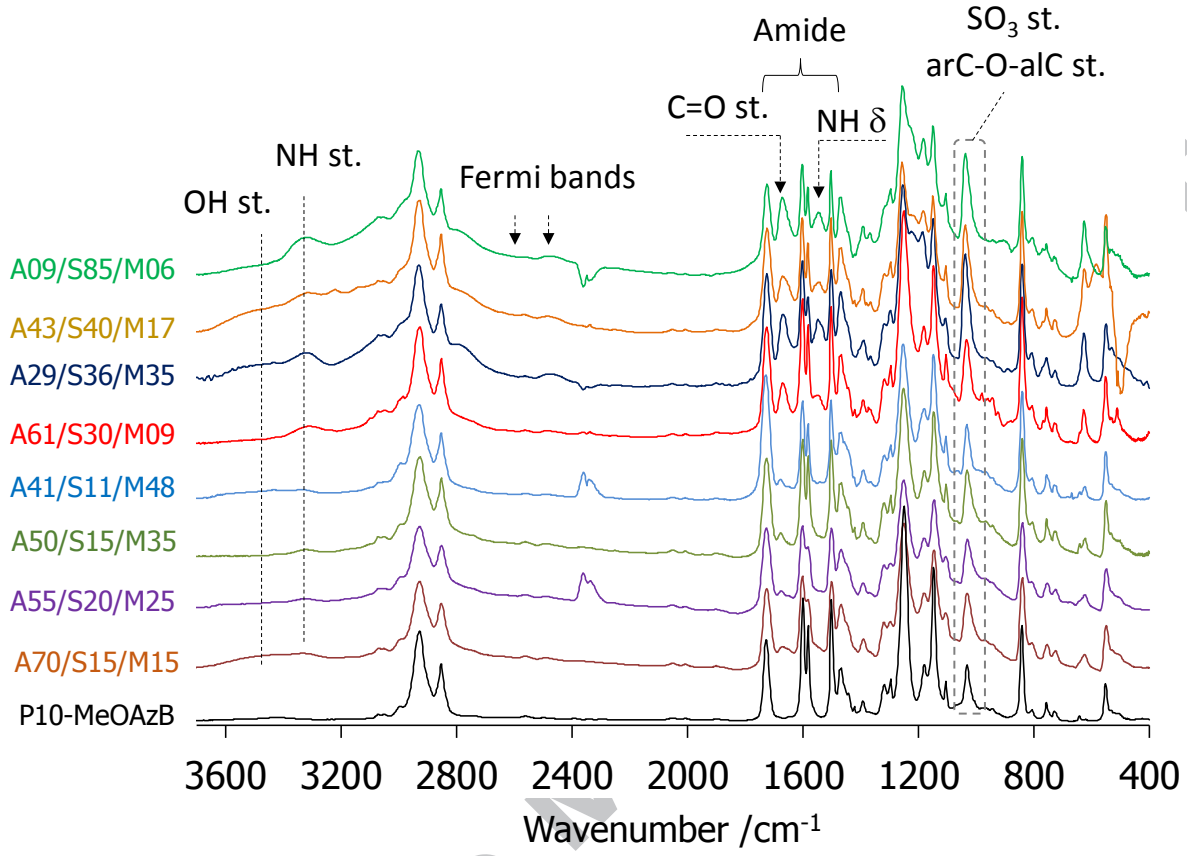

Figure 5. FT-IR spectra of the terpolymers, highlighting the contributions from the AMPS units. The Y-axis displays IR absorbance (*a.u.*) with the spectra shifted arbitrarily along this axis. *st.*, stretching; δ, bending.

Light responsive behaviour

We now turn our attention to the photo-responsive nature of the 10-MeOAzB/AMPS/MMA terpolymers, and discuss the dependence of the UV-visible spectra of THF solutions and films cast on ITO slides in **Figure 6**. As it was expected, the presence of 10-MeOAzB units induces light-responsive character in the terpolymers, assessed by UV-vis spectroscopy, and more specifically by the appearance of an intense band centred at ~362 nm, corresponding to the π–π* transition associated with the *E*-isomer of the azobenzene unit, and a weak absorption at ~450 nm, associated with the symmetric forbidden *n* - π* transition.[58] The

UV-visible spectra of the terpolymers show similar spectra to P10-MeOAzB, confirming that the photoresponsive character of the azobenzene units is maintained after copolymerisation. As expected, reducing the azobenzene content weakens the UV signals for the terpolymers, but otherwise their spectra are essentially identical, suggesting that the azobenzene moieties respond similarly to light exposure, see **Figure EIS4**.

Upon irradiating the solutions at 365 nm, the azobenzene units in the terpolymers undergo *trans*-to-*cis* photoisomerisation. The π–π* absorbance band in their UV-spectra decreases dramatically in intensity after exposure, whereas a slight increase in the intensity of the 450 nm region is observed, see **Figure 6(a)**. When the samples are kept in the dark, the intensity of the π–π* band increases with time, whereas that of the *n*–π* band decreases. After 24 hours, the original UV absorption spectra for all terpolymers are essentially recovered due to the thermally activated *cis*-to-*trans* relaxation.

The UV-spectra corresponding to the films also display the two previous main absorption regions, and during UV exposure there is a decrease of the π–π* band and a simultaneous increase of the *n*–π* band, see **Figure 6(b)**. This evidences that *trans*-to-*cis* photoisomerisation of the azobenzene groups is occurring in the films, even though longer exposure times were required to get a stationary state than in the solutions. Once UV-light exposure ceases, the UV spectra recover their original shapes, indicating *cis*-to-*trans* relaxation, again with lower rates than those observed for the solutions.

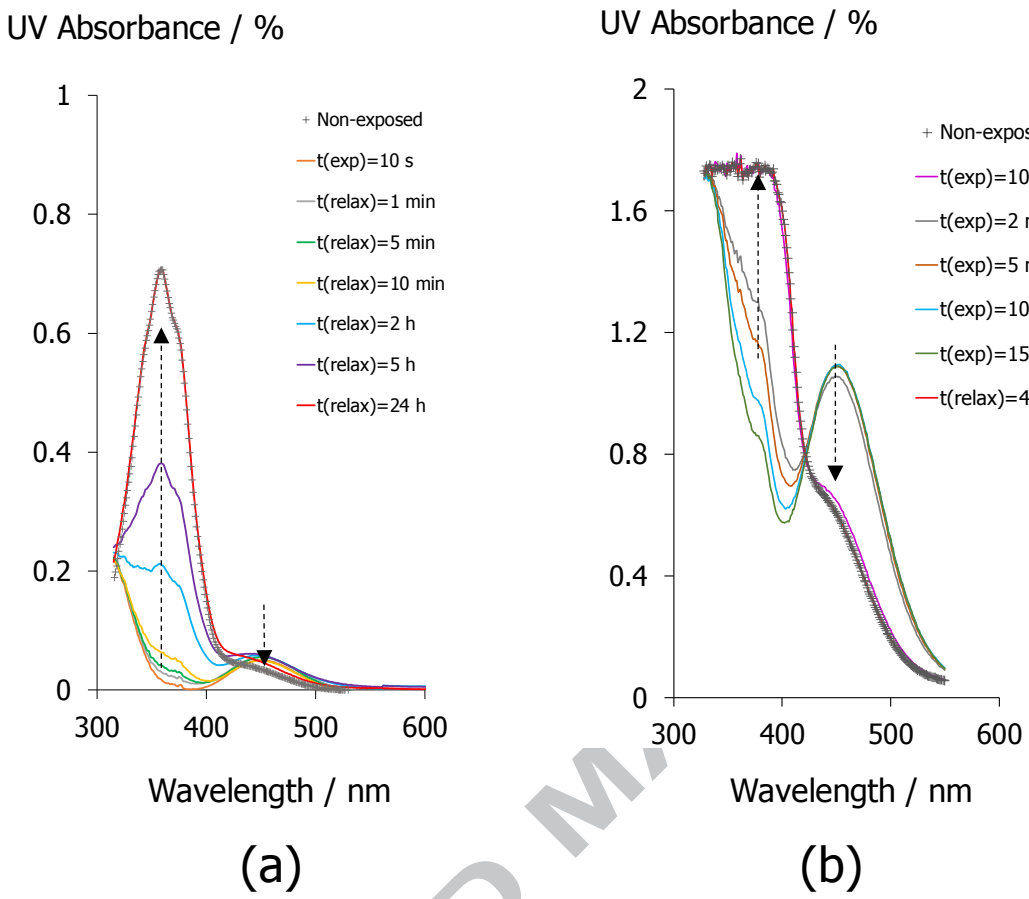

Figure 6. UV-visible spectra of A29/S36/M35, measured at room temperature, obtained for a: **(a)** 4.15 10^{-5} M THF solution; **(b)** film cast on ITO. Crosses correspond to the original spectrum prior to UV exposure (exp), and dotted arrows indicate the *cis*-to-*trans* thermal relaxation (relax) with time, *t*, after exposure and while keeping the samples in the dark.

Temperature-dependent conductivity

We now discuss the temperature dependence of the ionic conductivities for the 10-MeOAzB/AMPS/MMA terpolymers, measured using electrochemical impedance spectroscopy, EIS, in isothermal steps on cooling the samples from the isotropic melt. The occurrence of direct current, *dc*, conductivity, σ_{dc}, was detected from the Nyquist plots of the complex impedance, $Z^* = Z' + i\,Z''$, and more specifically by the appearance of a spike

with the real impedance axis, Z′ (see **Figure 7**, inset, and Figures **ESI6** and **ESI7**). The σ_{dc} values were obtained from plateaus of the real component of the complex conductivity, calculated as $\sigma' = \omega \cdot \varepsilon''$, when plotted as a function of the frequency, *f*, **Figure 7**, and the results are shown as Arrhenius plots in **Figure 8**.

Terpolymers with low AMPS contents do not exhibit appreciable *dc* conductivity and this suggests that a minimum threshold concentration of these groups is required to achieve charge transfer across these electrolytes. The presence of higher contents of AMPS groups in the side chains of the terpolymers promotes the appearance of plateaus in the log (σ') *vs* log(*f*) curves, indicative of long-range conductivity.

In the case of A61/S30/M09, A43/S40/M17 and A70/S15/M15, the plateaus in the conductivity plots are well-defined only above the glass transition, and it was not possible to obtain reliable values for σ_{dc} in the smectic glasses. Conductivities for these samples at high temperatures fall within the range 10^{-8} to 10^{-10} S·cm^{-1}. A09/S85/M06 and A29/S36/M35, on the other hand, exhibit considerably higher *dc* conductivity values than the rest of the terpolymers, between 10^{-4} to 10^{-8} S·cm^{-1}, and measurable in all the range of temperatures under study. Whereas the high conductivities for A09/S85/M06 could be somehow expected due to the high content of AMPS groups (~85 molar %),[59] the σ_{dc} values of A29/S36/M35 are surprisingly high, attributable to structural features of this particular terpolymer, in which the 10-MeOAzB, AMPS and MMA units are balanced.

The activation energies, E_a, for the direct current conductivity, σ_{dc}, were obtained from the Arrhenius plots in **Figure 8**, and the results are listed in **Table 3**. Samples show linear trends for log(σ_{dc}) in the liquid crystalline phases, giving E_a values within the range $60 - 83\ \text{kJ} \cdot \text{mol}^{-1}$. Above T_{LCI}, smaller activation energies are obtained, presumably due to a decreased viscosity of the isotropic melts. This effect can be considered analogous to

the rubbery to liquid transition observed in rubber-like polymers,[60] which is attributed to a decrease in the local viscosity due to removal of certain local interactions. In our case, the disappearance of the anisotropic interactions between mesogenic units at the clearing temperature may further enhance the conductivity of the 10-MeOAzB/AMPS/MMA terpolymers by an increase in their local mobility. The lowest activation energies were obtained for A09/S85/M06, whose Arrhenius plot displays a combination of two linear ranges, with the intersect coinciding with the glass transition of the terpolymer, T_g ~65°C.

In general terms, the absence of a rapid decrease in the σ_{dc} values on cooling towards the T_g of the terpolymers in **Figure 8**, precludes Vogel-Fulcher-Tammann (VFT) behaviour, and suggests that the conductivity is not strongly coupled to segmental motions of the terpolymers. The decoupled character of the conductivity may be explained by the occurrence of secondary relaxations located in the 10-MeOAzB side chains, which can activate motions near the backbone.[8, 61]

In the case of the amorphous A09/S85/M06, the presence of small amounts of mesogens may have a plasticizing effect and reduce the local viscosity expected by interactions between AMPS units, which is consistent with the low glass transition seen in **Table 2**. For A29/S36/M35, the activation energies are larger, and the conductivity values below T_{LCI} are lower than for A09/S85/M06, but these are still considerably high compared to other liquid crystalline polymers.[62-65] Even though these conductivities fall some orders of magnitude below the $\sigma_{dc} \sim 0.1\ S \cdot cm^{-1}$ range observed for non-mesogenic polymers containing, for example, poly(sulfonic) and poly(aromatic) backbones[66, 67], or benchmark polymeric electrolytes, such as Nafion[3] or poly(ethyelene oxide)[68], they present the opportunity to control ion transport by tuning their liquid crystalline phases. We observed, for example, how A29/S36/M35 can undergo a noticeable increase in conductivity upon irradiation with UV-light in its smectic phase, see **Figure ESI8**. This suggests that the presence of

azobenzenes in the *cis*-state by photoisomerisation may benefit ionic motions, perhaps by inducing local defects in the smectic structure of the terpolymer, in a similar fashion as moderate crosslinking degrees can promote conductivity by a decrease in local rigidity in smectic networks[62].

Table 3. Activation energies for *dc* conductivity in the 10-MeOAzB/AMPS/MMA terpolymers, Ea(σ_{dc}), calculated in the isotropic and smectic ranges.

Sample	**A*X*/S*Y*/M*Z***	**$E_a(\sigma_{dc})$ / kJ·mol^{-1}**	
		Isotropic	**Smectic**
#1	A70/S15/M15	58.9	82.3
#5	A61/S30/M09	48.5	-
#6	A29/S36/M35	60.1	66.3
#7	A43/S40/M17	-	64.3
#8	A09/S85/M06	24.0* 51.3**	

*T>80^{o}C, **T<80^{o}C

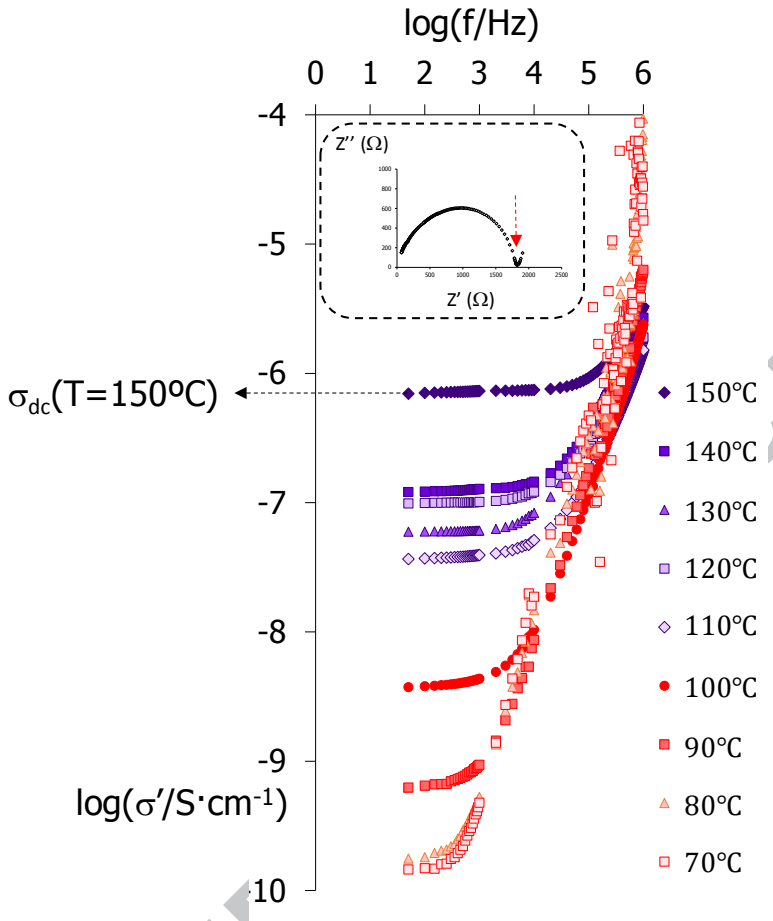

Figure 7. Double logarithmic plots of the real component, σ', of the complex conductivity of A29/S36/M35, $\sigma^*=\sigma'+ i\,\sigma''$, as a function of the frequency, measured in isothermal steps (ºC) on cooling from the isotropic melt, and estimation of σ_{dc} at T=150ºC. Dotted arrow in the inset shows the spike in the impedance Nyquist plot, indicative of *dc* conductivity.

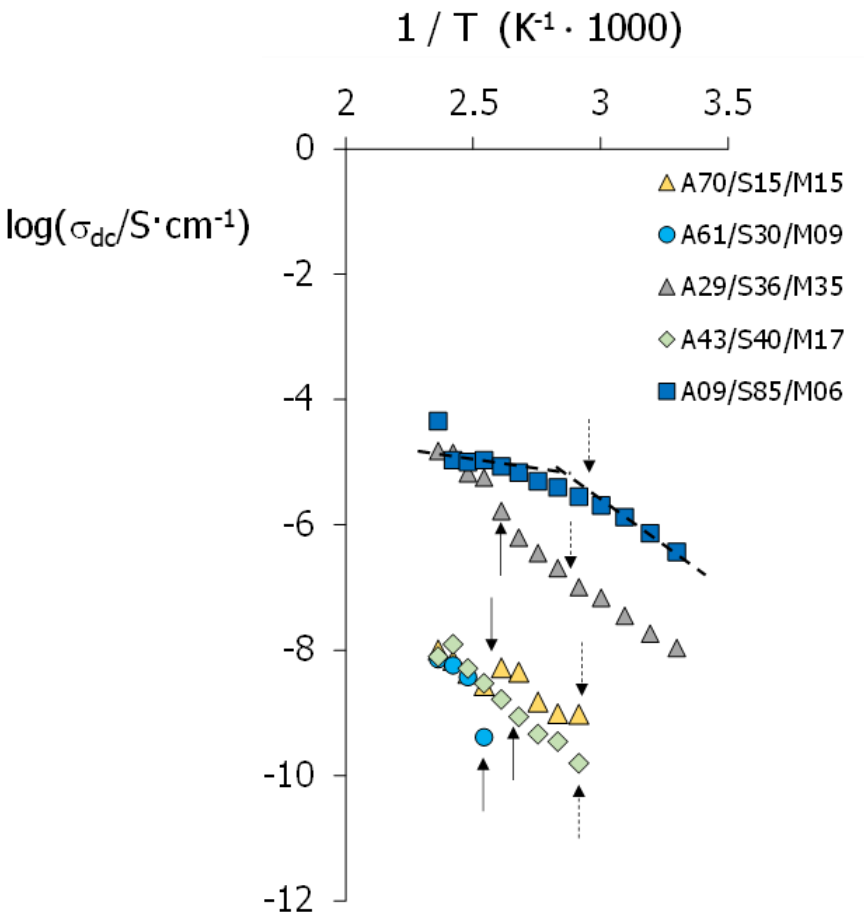

Figure 8. Arrhenius plots of the *dc* conductivity measured for the 10-MeOAzB/AMPS/MMA terpolymers. Dotted arrows indicate the glass transition temperatures, T_g, and solid arrows, clearing temperatures, T_{LCI}, taken from **Table 2**. Dotted lines represent the linear ranges for A09/S85/M06.

4. CONCLUSIONS

The 10-MeOAzB/AMPS/MMA terpolymers form smectic phases stabilised by microphase separation between polar and non-polar regions, even at surprisingly low concentrations of 10-MeOAzB mesogenic units. At sufficiently large contents of AMPS units, these form aggregates constrained between the smectic layers, resulting in *dc* conductivity in the terpolymers. The presence of MMA groups reduces the liquid crystal-isotropic transition temperature and liquid crystal range of the terpolymers by diluting the anisotropic interactions between 10-MeOAzB side-chains and by increasing T_g, respectively. Their presence, however, may also reduce the interactions between AMPS groups and increase free volume around the backbone. This latter effect, together with the formation of liquid crystalline phases, may contribute to increase the local mobility and ultimately promote decoupled ionic conductivity from segmental motions in the terpolymers.[69] The promising conductivity values obtained within the liquid crystal phases and the light responsive character, make the 10-MeOAzB/AMPS/MMA terpolymers attractive candidates as electrolytes whose transport properties can be optimised *via* their changes in their ultrastructure using external stimuli, and this is currently the focus of further studies to apply polarised light to create anisotropic conductivity pathways with high local ionic mobility.

ACKNOWLEDGMENTS. ARG and AMF thank the financial support of the Generalitat Valenciana, through the Grisolia and Forteza programs, and the Spanish Ministry of Science and Innovation, through the Research Projects ENE2007-67584-C03 and UPOVCE-3E-013 and the awarding of two FPI and FPU pre-doctoral grants. AMF and NFKA would like to thank the Royal Academy of Engineering for the award of the Newton Research Collaboration Programme grant NRCP1516/4/61. AMF acknowledges the School of Engineering of the University of Aberdeen for financial support.

DATA AVAILABILITY

The raw/processed data required to reproduce these findings cannot be shared at this time due to technical or time limitations.

REFERENCES

1. Schubert US. *Polymers for energy storage*. Polymer 2015;68:308-9.

2. Pereira EC, Cuesta A. *A personal perspective on the role of electrochemical science and technology in solving the challenges faced by modern societies*. Journal of Electroanalytical Chemistry. 2016;780:355-9.

3. Mauritz KA, Moore RB. *State of understanding of Nafion*. Chemical Reviews. 2004;104(10):4535-85.

4. Martinez-Felipe A, Imrie CT, Ribes-Greus A. S*pectroscopic and thermal characterization of the swelling behavior of nafion membranes in mixtures of water and methanol*. Journal of Applied Polymer Science. 2013;127(1):246-56.

5. Martinez-Felipe A. *Liquid crystal polymers and ionomers for membrane applications*. Liquid Crystals. 2011;38(11-12):1607-26.

6. Cho B. *Nanostructured organic electrolytes*. RSC Advances. 2014;4(1):395-405.

7. Stoeva Z, Lu Z, Ingram MD, Imrie CT. *A new polymer electrolyte based on a discotic liquid crystal triblock copolymer*. Electrochimica Acta. 2013;93:279-86.

8. Imrie CT, Ingram MD, McHattie GS. *Ion transport in glassy side-group liquid crystalline polymer electrolytes*. Advanced Materials. 1999;11(10):832.

9. Imrie CT, Ingram MD. *Bridging the gap between polymer electrolytes and inorganic glasses: Side group liquid crystal polymer electrolytes*. Molecular Crystals and Liquid Crystals. 2000;347:443-54.

10. Gao J, Wang Y, Norder B, Garcia SJ, Picken SJ, Madsen LA, Dingemans TJ. *Water and sodium transport and liquid crystalline alignment in a sulfonated aramid membrane*. Journal of Membrane Science. 2015;489:194-203.

11. Every HA, Mendes E, Picken SJ. *Ordered structures in proton conducting membranes from supramolecular liquid crystal polymers*. Journal of Physical Chemistry B. 2006;110(47):23729-35.

12. Montane X, Vilasrao Bhosale S, Antonio Reina J, Giamberini M. *Columnar liquid crystalline polyglycidol derivatives: A novel alternative for proton-conducting membranes*. Polymer. 2015;66:100-9.

13. Broer DJ, Bastiaansen CMW, Debije MG, Schenning APHJ. *Functional organic materials based on polymerized liquid-crystal monomers: Supramolecular hydrogen-bonded systems*. Angewandte Chemie-International Edition. 2012;51(29):7102-9.

14. van Kuringen HPC, Eikelboom GM, Shishmanova IK, Broer DJ, Schenning APHJ. *Responsive nanoporous smectic liquid crystal polymer networks as efficient and selective adsorbents*. Advanced Functional Materials. 2014;24(32):5045-51.

15. Li W, Kuang T, Jiang X, Yang J, Fan P, Zhao Z, Fei Z, Zhong M, Chang L, Chen F. *Photoresponsive polyelectrolyte/mesoporous silica hybrid materials with remote-controllable ionic transportation*. Chemical Engineering Journal. 2017;322:445-53.

16. Chen F, Jiang X, Kuang T, Chang L, Fu D, Yang J, Fan P, Zhong M. *Polyelectrolyte/mesoporous silica hybrid materials for the high performance multiple-detection of pH value and temperature*. Polymer Chemistry. 2015;6(18):3529-36.

17. Chen F, Jiang X, Kuang T, Chang L, Fu D, Yang Z, Yang J, Fan P, Fei Z, Zhong M. *Effect of nanoporous structure and polymer brushes on the ionic conductivity of poly(methacrylic acid)/anode aluminum oxide hybrid membranes*. RSC Advances. 2015;5(86):70204-10.

18. Elabd YA, Napadensky E, Sloan JM, Crawford DM, Walker CW. *Triblock copolymer ionomer membranes part I. methanol and proton transport*. Journal of Membrane Science. 2003;217(1-2):227-42.

19. Ye Y, Choi J, Winey KI, Elabd YA. *Polymerized ionic liquid block and random copolymers: Effect of weak microphase separation on ion transport*. Macromolecules. 2012;45(17):7027-35.

20. Kuan W, Remy R, Mackay ME, Epps,Thomas H.,,III. *Controlled ionic conductivity via tapered block polymer electrolytes*. RSC Advances. 2015;5(17):12597-604.

21. Choi UH, Lee M, Wang S, Liu W, Winey KI, Gibson HW, Colby RH. *Ionic conduction and dielectric response of poly(imidazolium acrylate) ionomers*. Macromolecules. 2012;45(9):3974-85.

22. Martinez-Felipe A, Lu Z, Henderson PA, Picken SJ, Norder B, Imrie CT, Ribes-Greus A. *Synthesis and characterisation of side chain liquid crystal copolymers containing sulfonic acid groups*. Polymer. 2012;53(13):2604-12.

23. Martinez-Felipe A, Imrie CT, Ribes-Greus A. *Study of structure formation in side-chain liquid crystal copolymers by variable temperature Fourier transform infrared spectroscopy*. Industrial & Engineering Chemistry Research. 2013;52(26):8714-21.

24. Martinez-Felipe A, Badia JD, Santonja-Blasco L, Imrie CT, Ribes-Greus A. *A kinetic study of the formation of smectic phases in novel liquid crystal ionogens*. European Polymer Journal. 2013;49(6):1553-63.

25. Matsui J, Miyata H, Hanaoka Y, Miyashita T. *Layered ultrathin proton conductive film based on polymer nanosheet assembly*. ACS Applied Materials & Interfaces. 2011;3(5):1394-7.

26. Sato T, Hayasaka Y, Mitsuishi M, Miyashita T, Nagano S, Matsui J. *High proton conductivity in the molecular interlayer of a polymer nanosheet multilayer film*. Langmuir 2015;31(18):5174-80.

27. Yabu H, Matsui J, Hara M, Nagano S, Matsuo Y, Nagao Y. *Proton conductivities of lamellae-forming bioinspired block copolymer thin films containing silver nanoparticles*. Langmuir. 2016;32(37):9484-91.

28. Pebalk D, Barmatov E, Shibayev V. *Liquid crystalline ionomers as a new class of mesomorphous polymeric systems*. Russian Chemical Reviews. 2005;74:555-76.

29. Nikonorova NA, Barmatov EB, Barmatova MV, Pebalk DA, Diaz-Calleja R. *Local modes of molecular mobility in comb-shaped liquid crystalline ionomers containing alkaline metal ions*. European Polymer Journal. 2008;44(11):3806-16.

30. Huang Y, Zhu M, Huang Y, Pei Z, Li H, Wang Z, Xue Q, Zhi C. *Multifunctional energy storage and conversion devices*. Advanced Materials. 2016;28(38):8344-64.

31. Poutanen M, Ikkala O, Priimagi A. *Structurally controlled dynamics in azobenzene-based supramolecular self-assemblies in solid state*. Macromolecules. 2016;49(11):4095-101.

32. Iamsaard S, Asshoff SJ, Matt B, Kudernac T, Cornelissen JJLM, Fletcher SP, Katsonis N. *Conversion of light into macroscopic helical motion*. Nature Chemistry. 2014;6(3):229-35.

33. Paterson DA, Xiang J, Singh G, Walker R, Agra-Kooijman DM, Martinez-Felipe A, Gan M, Storey JMD, Kumar S, Lavrentovich OD, et al. *Reversible isothermal twist-bend nematic-nematic phase transition driven by the photoisomerization of an azobenzene-based nonsymmetric liquid crystal dinner*. Journal of the American Chemical Society. 2016;138(16):5283-9.

34. Concellon A, Blasco E, Pinol M, Oriol L, Diez I, Berges C, Sanchez-Somolinos C, Alcala R. P*hotoresponsive polymers and block copolymers by molecular recognition based on multiple hydrogen bonds*. Journal of Polymer Science Part A-Polymer Chemistry. 2014;52(22):3173-84.

35. Chaganava I, Kilosanidze B, Kakauridze G, Oriol L, Pinol M, Martinez-Felipe A. *Induction of the vector polyphotochromism in side-chain azopolymers*. Journal of Photochemistry and Photobiology A: Chemistry. 2017;354:70-7.

36. Chaganava I, Kilosanidze B, Kakauridze G, Oriol L, Pinol M, Martinez-Felipe A. *Photoanisotropy in polarization-sensitive polymer materials based on the media with covalently-bonded components*. Organic Photonic Materials and Devices Xix. 2017;10101:UNSP 101010T.

37. Imrie C, Karasz FE, Attard GS. *The effect of molecular-weight on the thermal-properties of polystyrene-based side-chain liquid-crystalline polymers*. Journal of Macromolecular Science-Pure and Applied Chemistry. 1994;A31(9):1221-32.

38. Craig A, Imrie C. *Effect of spacer length on the thermal-properties of side-chain liquid-crystal poly(methacrylate)s*. Journal of Materials Chemistry. 1994;4(11):1705-14.

39. Schleeh T, Imrie CT, Rice D, Karasz FE, Attard GS. U*ltrastructure studies of polystyrene-based side-chain liquid-crystalline copolymers containing charge-transfer groups*. Journal of Polymer Science Part A-Polymer Chemistry. 1993;31(7):1859-69.

40. Martinez-Felipe A, Lu Z, Henderson PA, Picken SJ, Norder B, Imrie CT, Ribes-Greus A. *Synthesis and characterisation of side chain liquid crystal copolymers containing sulfonic acid groups*. Polymer. 2012;53(13):2604-12.

41. Mohan DJ. *Synthesis, characterization and swelling properties of copolymers of N(-1,1-dimethyll-3-oxobutyl)acrylamide with methyl methacrylate*. Designed Monomers and Polymers. 2014;17(5):438-44.

42. Aguilar M, Gallardo A, Fernandez M, San Roman J. *In situ quantitative H-1 NMR monitoring of monomer consumption: A simple and fast way of estimating reactivity ratios*. Macromolecules. 2002;35(6):2036-41.

43. Mishra A, Choudhary V. *Synthesis, characterizations and thermal behavior of methyl methacrylate and N-(p-carboxyphenyl) methacrylamide/arylamide copolymers*. Journal of Applied Polymer Science. 2000;78(2):259-67.

44. Talpur M, Oracz P, Kaim A. S*tudy of methyl methacrylate-acrylamide copolymerization system in cyclohexanone in the absence of conventional radical initiator*. Polymer. 1996;37(18):4149-54.

45. Ferriol M, Gentilhomme A, Cochez M, Oget N, Mieloszynski J. *Thermal degradation of poly(methyl methacrylate) (PMMA): Modelling of DTG and TG curves*. Polymer Degradation and Stability. 2003;79(2):271-81.

46. Wang Y, Ma X, Zhang Q, Tian N. *Synthesis and properties of gel polymer electrolyte membranes based on novel comb-like methyl methacrylate copolymers*. Journal of Membrane Science. 2010;349(1-2):279-86.

47. Li G, Zhao C, Li X, Qi D, Liu C, Bu F, Na H. *Novel side-chain-type sulfonated diphenyl-based poly(arylene ether sulfone)s with a hydrogen-bonded network as proton exchange membranes*. Polymer Chemistry. 2015;6(32):5911-20.

48. Cook AG, Inkster RT, Martinez-Felipe A, Ribes-Greus A, Hamley IW, Imrie CT. *Synthesis and phase behaviour of a homologous series of polymethacrylate-based side-chain liquid crystal polymers*. European Polymer Journal. 2012;48(4):821-9.

49. Fryer D, Peters R, Kim E, Tomaszewski J, de Pablo J, Nealey P, White C, Wu W. *Dependence of the glass transition temperature of polymer films on interfacial energy and thickness*. Macromolecules. 2001;34(16):5627-34.

50. Imrie CT, Schleeh T, Karasz FE, Attard GS. *Dependence of the transitional properties of polystyrene-based side-chain liquid-crystalline polymers on the chemical nature of the mesogenic group*. Macromolecules. 1993;26(3):539-44.

51. Martinez-Felipe A, Cook AG, Wallage MJ, Imrie CT. *Hydrogen bonding and liquid crystallinity of low molar mass and polymeric mesogens containing benzoic acids: A*

variable temperature Fourier transform infrared spectroscopic study. Phase Transitions. 2014;87(12):1191-210.

52. Martinez-Felipe A, Imrie CT. *The role of hydrogen bonding in the phase behaviour of supramolecular liquid crystal dimers*. Journal of Molecular Structure. 2015;1100:429-37.

53. Martinez-Felipe A, Cook AG, Abberley JP, Walker R, Storey JMD, Imrie CT. *An FT-IR spectroscopic study of the role of hydrogen bonding in the formation of liquid crystallinity for mixtures containing bipyridines and 4-pentyloxybenzoic acid*. RSC Advances. 2016;6:108164-79.

54. Odinokov SE, Iogansen AV. T*orsional gamma-(OH) vibrations, fermi resonance 2gamma-(OH) -- NU-isotopic effects in IR-spectra of h-complexes of carboxylic-acids with strong bases*. Spectrochimica Acta Part A-Molecular Spectroscopy. 1972;A 28(12):2343-50.

55. Percec V, Hahn B. *Liquid-crystalline polymers containing heterocycloalkanediyl groups as mesogens .7. molecular-weight and composition effects on the phase-transitions of poly(methylsiloxane)s and poly(methylsiloxane-co-dimethylsiloxane)s containing 2-[4-(2(s)-methyl-1-butoxy)phenyl]-5-(11-undecanyl)-1,3,2-dioxaborinane side groups*. Macromolecules. 1989;22(4):1588-99.

56. Percec V, Hahn B, Ebert M, Wendorff J. *Liquid-crystalline polymers containing heterocycloalkanediyl groups as mesogens .8. morphological evidence for microphase separation in poly(methylsiloxane-co-dimethyl-siloxane)s containing 2-[4-(2(s)-methyl-1-butoxy)-phenyl]-5-(11-undecanyl)-1,3,2-dioxaborinane side groups*. Macromolecules. 1990;23(7):2092-5.

57. Percec V, Lee M. *Molecular engineering of liquid-crystalline polymers by living polymerization .20. synthesis and characterization of binary copolymers of [11-(4'-cyanobiphenyl-4-yloxy)undecanyloxy]ethylene with normal-butyl vinyl ether, and of 2-[(4'-cyanobiphenyl-4-yl)oxy]ethyl vinyl ether with (normal-butoxy)ethylene*. Journal of Materials Chemistry. 1992;2(6):617-23.

58. Kumar G, Neckers D. *Photochemistry of azobenzene-containing polymers*. Chemical Reviews. 1989;89(8):1915-25.

59. Coelho R. *On the static permittivity of dipolar and conductive media - an educational-approach*. Journal of Non Crystalline Solids. 1991;131:1136-9.

60. Angell C, Imrie C, Ingram M. *From simple electrolyte solutions through polymer electrolytes to superionic rubbers: Some fundamental considerations*. Polymer International. 1998;47(1):9-15.

61. McHattie GS, Imrie CT, Ingram MD. *Ionically conducting side chain liquid crystal polymer electrolytes*. Electrochimia Acta. 1998;43(10-11):1151-4.

62. Liang T, van Kuringen HPC, Mulder DJ, Tan S, Wu Y, Borneman Z, Nijmeijer K, Schenning APHJ. A*nisotropic dye adsorption and anhydrous proton conductivity in smectic liquid crystal networks: The role of cross-link density, order, and orientation*. ACS Applied Materials & Interfaces. 2017;9(40):35218-25.

63. Yang X, Tan S, Liang T, Wei B, Wu Y. *A unidomain membrane prepared from liquid-crystalline poly(pyridinium 4-styrene sulfonate) for anhydrous proton conduction*. Journal of Membrane Science. 2017;523:355-60.

64. Kobayashi T, Ichikawa T, Kato T, Ohno H. *Development of glassy bicontinuous cubic liquid crystals for solid proton-conductive materials*. Advanced Materials. 2017;29(4):1604429.

65. Concellon A, Liang T, Schenning APHJ, Luis Serrano J, Romero P, Marcos M. *Proton-conductive materials formed by coumarin photocrosslinked ionic liquid crystal dendrimers*. Journal of Materials Chemistry C. 2018;6(5):1000-7.

66. Yuan S, Guo X, Aili D, Pan C, Li Q, Fang J. *Poly(imide benzimidazole)s for high temperature polymer electrolyte membrane fuel cells*. Journal of Membrane Science. 2014;454:351-8.

67. Yang J, Wang Y, Yang G, Zhan S. *New anhydrous proton exchange membranes based on fluoropolymers blend imidazolium poly (aromatic ether ketonejs for high temperature polymer electrolyte fuel cells*. International Journal of Hydrogen Energy. 2018;43(17):8464-73.

68. Luntz AC, McCloskey BD. *Nonaqueous li-air batteries: A status report*. Chemical Reviews. 2014;114(23):11721-50.

69. Kim O, Jo G, Park YJ, Kim S, Park MJ. *Ion transport properties of self-assembled polymer electrolytes: The role of confinement and interface*. Journal of Physical Chemistry Letters. 2013;4(13):2111-7.

Ionically conducting and photoresponsive liquid crystalline terpolymers: towards multifunctional polymer electrolytes.
by Laura Vanti et al.

Highlights

New side-chain terpolymers contain mesogenic, light-responsive and polar groups
Terpolymers show liquid crystal smectic behaviour in a broad range of compositions
Polar groups confined between smectic layers can act as anisotropic ionic pathways
Balanced compositions of the monomers promote liquid crystallinity and conductivity
Terpolymers show signs of ionic mobility decoupled from polymer segmental motions

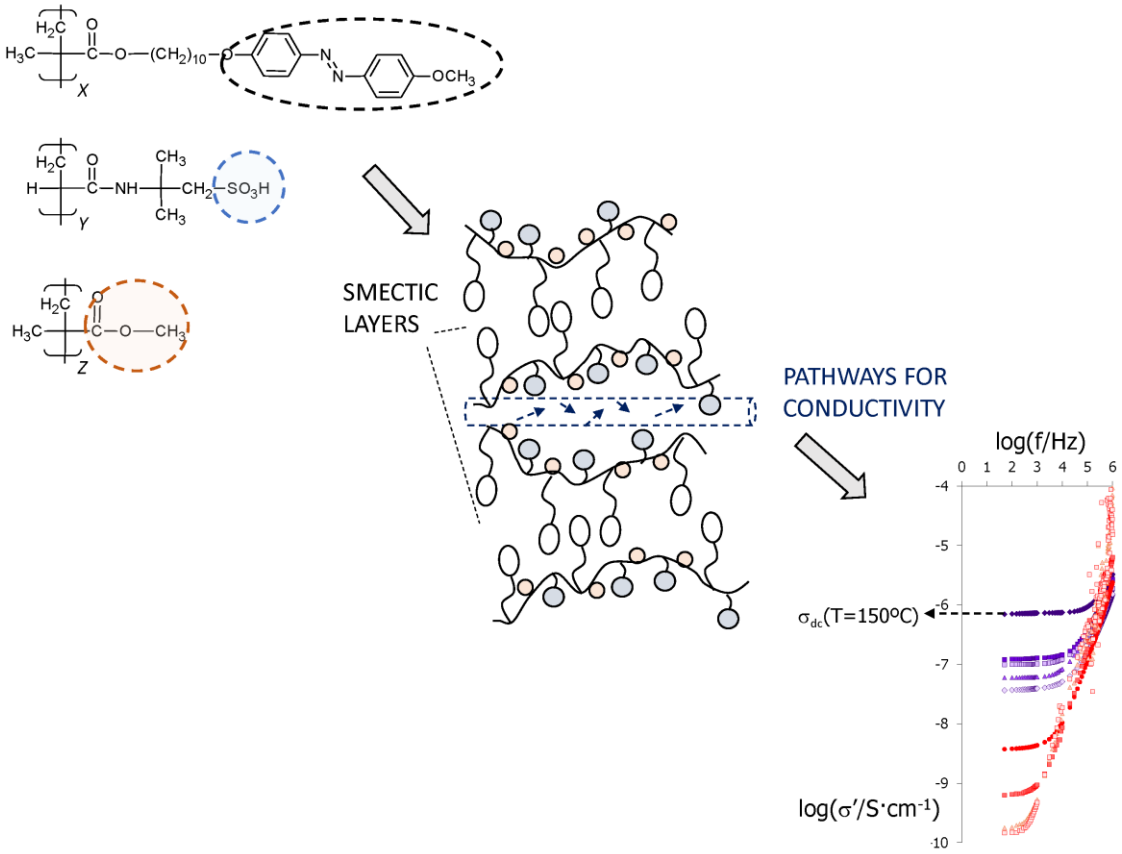
SMECTIC
LAYERS
PATHWAYS FOR
CONDUCTIVITY
log(f/Hz)
σdc(T=150ºC)
log(σ'/S·cm-1)